ENGINEERING RESEARCH JOURNAL (ERJ)
Vol. 1, No. 41 July. 2019, pp. 51-62
Journal Homepage: www.feng.bu.edu.eg

The Performance Enhancement of a Water Chiller of Conically Coiled Tube Evaporator

H.A. El-Gammal, M.R. Salem, A.A. Abdulaziz and K.M. Elshazly
Mechanical Engineering Department, Faculty of Engineering at Shoubra, Benha University.

Abstract. The present work experimentally investigates the effect of the geometrical parameters of a conically coiled tube in tube (CCTIT) evaporator and its operating conditions on the coefficient of performance (COP) of a vapour compression refrigeration system (VCRS). The CCTIT evaporator is oriented vertically, through which refrigerant R134a flows in its internal tube, while pure water flows in its annulus as heating mediums, in a counter-flow configuration. Twelve CCTIT evaporators with different taper angles (0°–135°) and pitch ratios (0.0777–0.1311) are constructed. Totally 72 test runs are performed on the twelve evaporators for heating water flow rates from 1.8 to 14 l/min, which are equivalent to Dean number in the evaporator annulus from 119.8 to 756.4. The experimental results demonstrate that increasing the taper angles and the pitch ratio of the CCTIT evaporator in addition to decreasing the $De_{ev,w}$ augments both the COP of the VCRS. Finally, an experimental correlation is developed to predict the COP of the VCRS as a function of the investigated parameters.

Keywords: Experimental, Conically coiled tube, Coefficient of performance, Vapour compression refrigeration system, Taper angle, Pitch.

1. INTRODUCTION

Enhancing the thermal performance of the refrigeration systems affects directly on the energy, material and cost savings. The VCRS is one of the refrigeration systems, which is used in most domestic refrigerators in addition to in numerous large industrial and commercial refrigeration systems [1]. There are numerous methods that were employed in the VCRS to improve its COP. One of the proposed methods for improving the heat exchange is the helically coiled tubes (HCTs). They are widely used as heat exchangers and have many applications. This wide application of the HCTs is due to their compactness and the geometry promotes good mixing of the fluids, which leads to increasing the heat transfer coefficients [2, 3]. Due to the extensive use of the HCTs in these applications, knowledge about the heat transfer and pressure drop characteristics is very important. A schematic representation of HCT characteristics with main geometrical parameters is shown in Fig. 1. Considering any cross-section of the HCT created by a plane passing through the coil axis, the side of tube wall nearest to the coil axis is termed inner side of the coil, while the farthest side is labelled as the outer side of the coil.

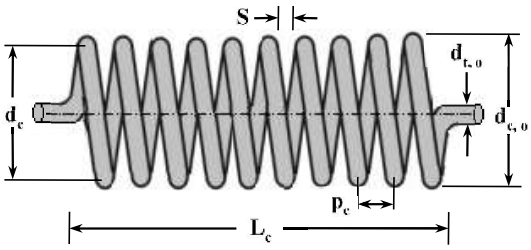

Fig. 1: Basic geometry of a HCT.

There are also dimensionless parameters that were commonly used to explain the effects of the coil curvature and coil torsion. They are defined as follows [4, 5]:

$$\delta = \frac{d_{t,i}}{d_c} \quad (1)$$

$$\lambda = \frac{p_c}{\pi d_c} \quad (2)$$

Where

δ Coil curvature ratio; it is the ratio of the inner diameter of the coiled tube ($d_{t,i}$) to the mean diameter of the coil curvature, d_c.

λ Coil torsion (pitch ratio); it is the ratio of the coil pitch (p_c) to the established length of one turn of the coil (πd_c).

There are numerous studies, which were carried out enhance the COP of the VCRS. Some of them investigated the effect of employing liquid-suction heat exchanger [6–11] into the VCRS. Other studies devoted to investigate the effect of geometrical parameters of the capillary tube on the VCRS performance [12–21]. In other investigations, the effect of adding nanoparticles to the VCRS refrigerant or compressor oil was examined [22–34]. Other investigations considered the evaporator/condenser geometry. Prasonna and Kishore [35]practically examined the effect of employing a shell and coil heat exchanger between the compressor and the condenser of a simple VCRS on its performance. It was revealed a significant decrease in the evaporation temperature, and therefore the COP of the cycle was augmented by 16%, while the mass flow of the refrigerant and the power required to drive the compressor were reduced by 14%. Chandramouli et al. [36] performed an experimental investigation on the COP of a domestic refrigerator by incorporating an evaporator of a spiral coil shape. The results demonstrated that the refrigeration effect and COP of the cycle were augmented by 1.5% due to using the proposed design. Kumar et al. [37] experimentally compared the effect of a conventional serpentine condenser with a spiral shape on the COP of a domestic refrigerator. The results indicated that the spiral coil condenser provided a maximum COP of 4.25 with 18.8% more than the conventional one. Vali et al. [38] practically tested the performance of a simple domestic refrigerator for two designs of the condenser; conventional serpentine type and HCT type. R134a was used as the working refrigerant. The results indicated that using a helically coiled condenser augmented the cycle COP by 21.4%. Patil et al. [39] experimentally and numerically carried out an effective analysis to compare the COP of a VCRS for employing a conventional condenser and for a spiral micro tube air cooled condenser. The results demonstrated that there was a decrease in the compressor work by 35.9%, which resulted in an enhancement in the COP by 13.45% with conducting the spiral condenser.

From the literature survey, it is clear that there are numerous techniques that were conducted to enhance the COP of the VCRSs. However, there is still a need for the COP improvement. One of the proposed techniques is the HCT, which enhanced the thermal performance of the heat exchangers examined by other researchers. As indicated, the geometrical parameter of the coiled tubes and the operating conditions of the VCRS affect its COP. It was demonstrated that decreasing the coil curvature increased the rate of heat transfer rate in addition to the pressure drop. Therefore, in the present study, it is aimed to investigate the effect of the geometrical parameters of coiled tubes with different taper angles and coil torsions on the performance attributes of the refrigeration cycle at different operating condition.

2 Experimental apparatus

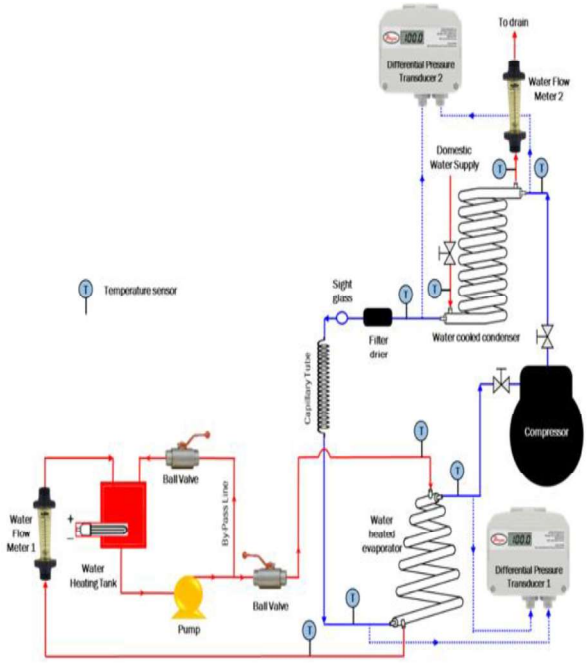

Fig. 2: Schematic diagram of the experimental setup.

The apparatus used in the present investigation comprisesheating and cooling water loops along with the refrigerant circuit. The hot water (supplied to the annulus side of the VCRS evaporator) circuit consists of a heating unit with a thermostat, pump, valves, water flow meter and the connecting pipes. While the cooling water supplied to the annulus side of the VCRS condenser from the domestic water supply is passed through the connecting pipes and is controlled by a valve and water flow meter through an open loop. In addition, the refrigerant

circuit consists of a compressor, valves, HCTIT condenser, filter drier, sight glass, capillary tube, CCTIT evaporator, temperature sensors, pressure/pressure difference transducers and the connecting pipes. Fig. 2 is a schematic representation of the experimental facility in which the heating water from the heating unit to/from the evaporator annulus, and the cooling water to/from the condenser annulus is revealed as red lines, while the refrigerant (R134a) in the VCRS is illustrated with blue lines.

Thirteen CCTIT evaporators of counter-flow configuration are constructed with different taper angles and coil torsions. The characteristic dimensions of the tested coils are revealed in Table 1. In the experimental runs, twelve of them (coils no. 1 to 12) are used as evaporators while the coil no. 13 is used as the condenser. The CCTITs are formed from straight soft copper tubes of the same length 5000 mm. The inner tube is of inner ($d_{t,i}$) and outer ($d_{t,o}$) diameters of 8.31 mm and 9.52 mm, respectively, while the outer tube is of inner ($d_{an,i}$) and outer ($d_{an,o}$) diameters of 17.65 mm and 19.05 mm, respectively. In addition, the coils are formed with four different taper angles (θ); 0° (helical), 45°, 90° and 135°. Furthermore, the first (top) turn of all coils is of an inner coil diameter of 100 mm, while the final (base) turn is of a different diameter according to the coil taper angle. It ought to be noticed that for CCTITs of θ = 0°, the pitch between the coil turns is the same, while for other angles, the pitch increments as the coil turn diameter increases to provide the same torsion for all turns as indicated in Eq. (2). In addition, expanding the cone angle leads to decrease the total number of coil turns due to the fixed length of the tube as illustrated in Table 1.

Additionally, to prevent any flattening to the CCTITs during coiling process, the tubes are filled with fine sand before bending to safeguard the smoothness of the inward surface and this is washed with high hot water flow after the process. Furthermore, care is taken to locate the inner tube into the center of the outer tube by using a circular ring that has the dimension of the annulus with a clearance of 0.5 mm during the filling progression. As the annulus is filled with fine sand, the ring is moved systematically until it exits from the other end of the tube after the annulus is completely loaded with the fine sand.

Table 1: Characteristic dimensions of the tested coils.

CoilNo.	TaperAngle (θ)	$p_{c,1}$(mm)	λ	N	L_c(mm)
1	0°	29.05	0.0777	15.92	462.35
2		39.05	0.1044		780.66
3		49.05	0.1311		1098.97
4	45°	29.05	0.0777	6.47	392.70
5		39.05	0.1044	5.57	471.70
6		49.05	0.1311	4.96	549.90
7	90°	29.05	0.0777	4.19	318.40
8		39.05	0.1044	3.60	370.30
9		49.05	0.1311	3.31	428.50
10	135°	29.05	0.0777	2.74	231.20
11		39.05	0.1044	2.19	277.70
12		49.05	0.1311	2.15	343.80
13	0°	39.05	0.1044	15.92	780.66

Additionally, two copper pipes of inner diameter of 17.65 mm are welded at the outer tube to permit the water to enter/exit to/from the annular passage. Moreover, the outer surface of the CCTIT evaporators/condensers is thermally isolated with a rubber insulation material (12.4 mm thickness). Fig. 3 reveals a photograph of the CCTIT evaporator/condenser.

Fig. 3: A photograph and schematic representation of the CCTIT evaporator/condenser.

In the present VCRS, a 1 hp centrifugal compressor model (KCG498HAG-C221H) is used. Additionally, a narrow copper tube of 1.62 mm internal diameter and 1500 mm effective length is conducted as a capillary device. Two digital pressure/differential pressure transducers are employed for measuring the pressure and pressure difference of the refrigerant at the evaporator/condenser inlets and exits. One of them is of a high scale (installed at the inlet and exit of the condenser) with a differential pressure range of 0–206.8 kPa, with a maximum pressure of 17.24 bar. While the other transducer of a lower scale (installed at the inlet and exit of the evaporator) with a differential pressure range of 0–103.4 kPa, with a maximum pressure of 3.45 bar. Both transducers are liquid and gas pressure measurement and of accuracy of ±1% of full scale.Four temperature sensors of digital readers

with a resolution of 0.1°C are utilized to measure the temperatures of the refrigerant incoming or leaving the condenser and the evaporator. The sensors are conducted on the refrigerant copper tube. Disregarding the conduction resistance of the tube wall, the readings are presumed to equal the refrigerant temperatures at these locations. The used filter drier and sight glass are Danfoss Type. The size of their inlet and outlet tubes is 3/8 inch.

For the heating unit, it is comprised of stainless steel slab (2 mm thickness), which is formed to produce a cabinet with dimensions of 300 mm * 300 mm * 600 mm. Three ports are conducted to the cabinet; one is at the tank base, which represents the departure pipe to the pump. Whilst the others are on the cover of the tank, which represent the inlet ports from the evaporator and from the by-pass line. Two electric heaters (have a maximum power of 6 kW) are installed horizontally at the bottommost of the heating cabinet to heat the water to the wanted temperature. The operation of the electric heaters is based on a pre-adjusted digital thermostat, which is used to keep a constant temperature of the water directed to the evaporator. Moreover, the outer sides of the tank is thermally isolated utilizing a layer of each of ceramic fiber and glass wool. The heating water is given from the heating unit and circulated through the annular passage of the evaporator, flow meter-1 and is backed to the heating tank. The water is delivered by a 0.5 hp power rating centrifugal pump with a maximum capacity of 30 l/min. Two identical variable area flow meters of a range from 1.8 to 18 l/min (accuracy of ±5% of reading), are used to amount the rate of the heating/cooling water flow required for the evaporator/condenser. Four digital sensors, with a resolution of 0.1°C, are directly embedded into the flow streams, at approximately 50 mm from inlet and exit ports of the annulus of the evaporator and condenser, to measure the water temperatures. While for the cooling loop, the cooling water circuit is an open loop. It is provided from the domestic water source and supplied to the annular passage of the condenser then to the drain. The rate of water flow is specified by a valve and flow meter-2.

3 Experimental Procedures

To initiate the experiments, the following parts are assembled: the evaporator, compressor, condenser, filter drier, sight glass, capillary tube, heating tank, pump, piping, flow meters, valves and the pressure transducers. These parts are connected together using either nuts or welding the pipes with silver solder. Then, the temperature sensors are attached on the refrigeration piping at evaporator/condenser inlets and outlets, in addition to four temperature sensors are inserted in evaporator/condenser water inlets and outlets to measure the heating and cooling water inlet ant outlet temperatures. After attaching the temperature sensors on the refrigerant tubes, they are well isolated from the surroundings. After assembling the VCRS components, it is charged with R134a.

The first step to collect the data from the system is to fill the heating tank with water from the domestic water supply, and then the electric heaters, the compressor, and the pump are turned on. The temperature of the heating water in the tank is adjusted at 20±0.5°C by regulating the temperature of the heating tank through its thermostat. While the condenser annulus is linked to the tap of the domestic water supply through a flexible hose. The water from the heating tank is circulated in the main line to the evaporator annulus at different flow rates in each experiment. The remainder from the pumped flow is returned to the tank through a bypass line. The range of the operating conditions are revealed in Table 2.

Table 2: Range of operating conditions.

Component	Shape	Parameters	Range or value
Evaporator	CCTIT	Coiled tube torsion	0.0777–0.1311
		Taper angle, °	0, 45, 90, 135
		Heating water flow rate, l/min	1.8–14
		Heating water inlet temperature, °C	20
		Heating water Dean Number	119.8–756.4
Condenser	HCTIT	Coiled tube torsion	0.1044
		Taper angle, °	0
		Cooling water flow rate, l/min	6
		Cooling water inlet temperature, °C	28
		Cooling water Dean Number	$De_{c,ave} \cong 630.4$

In addition, all experiments are conducted with cooling water entering the condenser annulus at 28±1°C inlet temperature. While its flow rate is adjusted through the faucet handle and the flow meter 2. A series of 72 experiments are carried out on the twelve evaporator geometries shown in Table 1. During the test operation, the steady-state condition is conducted when a maximum variation of 0.5°C for each temperature sensor reading within 20 minutes is recorded. Moreover, it is considered to be achieved when the stable fluid inlet and outlet temperatures are obtained; variation of inlet and outlet temperatures of the water and refrigerant streams are within 0.2°C

during a minute period before each measurement is taken.

4 Data Reduction

The measured temperatures and pressures during the experiments are used to calculate the specific enthalpy of the refrigerant in the different locations of the VCRS. It should be noted that each experiment is repeated three times, and the average readings of the measured variables are recorded despite the tinny difference between these repeated readings. Microsoft Excel sheets are prepared to process the experimental data for the COP and the other characteristic parameters of the VCRS. The specific enthalpy of the refrigerant is estimated using its measured pressure and temperature at evaporator and condensers inlet end exit. Schematic representation of the VCRS on the P-h chart is revealed in Fig. 4. The estimated specific enthalpies are used for calculating the following parameters:

$$RE = h_1 - h_4 \quad (3)$$

$$w_c = h_2 - h_1 \quad (4)$$

$$q_c = h_2 - h_3 \quad (5)$$

$$COP = \frac{RE}{w_c} = \frac{h_1 - h_4}{h_2 - h_1} \quad (6)$$

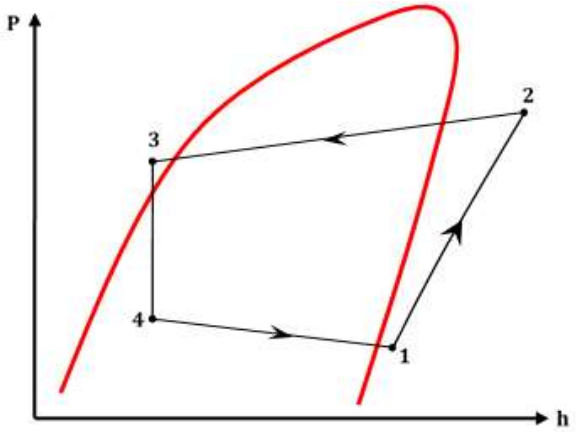

Fig. 4: Schematic representation of the VCRS on the P-h chart.

It should be noticed that the specific enthalpy of the R134a entering the evaporator (h_4) is assumed to be equal to the specific enthalpy of the refrigerant entering the capillary tube (h_3). In addition, to calculate refrigerant mass flow rate in the VCRS, the compressor power is calculated by measuring the voltage drop and current passing across it.

$$\dot{m}_{ref} = \frac{W_c}{w_c} = \frac{IV\cos\emptyset}{h_2 - h_1} \quad (7)$$

According to Ministry of Electricity and Energy in Egypt, the power factor, $\cos\emptyset$, for the public network is ranged from 0.93 to 0.97. In the present study, the AC power factor is assumed to be 0.95. Additionally, to ensure the veracity of the measured data and calculations, the evaporator heat transfer rate is calculated from refrigerant and heating water data as follows:

$$\dot{Q}_{ev,ref} = \dot{m}_{ref} \cdot RE = \dot{m}_{ref}(h_1 - h_4) \quad (8)$$

$$\dot{Q}_{ev,w} = \dot{m}_{ev,w} Cp_{ev,w}(T_{ev,w,i} - T_{ev,w,o}) \quad (9)$$

With the same method, the condenser load is calculated;

$$\dot{Q}_{c,ref} = \dot{m}_{ref} q_c = \dot{m}_{ref}(h_2 - h_3) \quad (10)$$

$$\dot{Q}_{c,w} = \dot{m}_{c,w} Cp_{c,w}(T_{c,w,o} - T_{c,w,i}) \quad (11)$$

Assuming that the measurements are sufficiently accurate without heat gain or loss, there is an energy balance between the two streams $Q_{ev,ref} = Q_{ev,w}$ and $Q_{c,ref} = Q_{c,w}$. While in the real experiments, there would always be some discrepancy between the two rates. Therefore, the arithmetical mean of the two, $Q_{ev,ave}$ and $Q_{c,ave}$ can be used as the heat load of each exchanger.

$$Q_{ev,ave} = \frac{Q_{ev,ref} + Q_{ev,w}}{2} \quad (12)$$

$$Q_{c,ave} = \frac{Q_{c,ref} + Q_{c,w}}{2} \quad (13)$$

$$\Delta Q_{ev} = \frac{|Q_{ev,w}| - |Q_{ev,ref}|}{Q_{ev,ave}} \quad (14)$$

$$\Delta Q_c = \frac{|Q_{c,ref}| - |Q_{c,w}|}{Q_{c,ave}} \quad (15)$$

For all experimental tests, the water and refrigerant loads in the evaporator and the condenser did not differ by more than ±2.2% and ±3%, respectively. For the water Dean Number in the evaporator ($De_{ev,w}$) annulus is calculated as follows;

$$De_{ev,w} = Re_{ev,w}(\delta_{an})^{0.5} = \frac{4\,\dot{m}_{ev,w}}{\pi\, d_{an,h}\mu_{ev,w}}\left(\frac{d_{an,h}}{d_c}\right)^{0.5} \quad (16)$$

5 Results and Discussions

5.1 Operating Conditions

Fig. 5 presents the obtained results due to varying the CCTIT evaporator taper angle and torsion in addition to its heating water Dean Number.

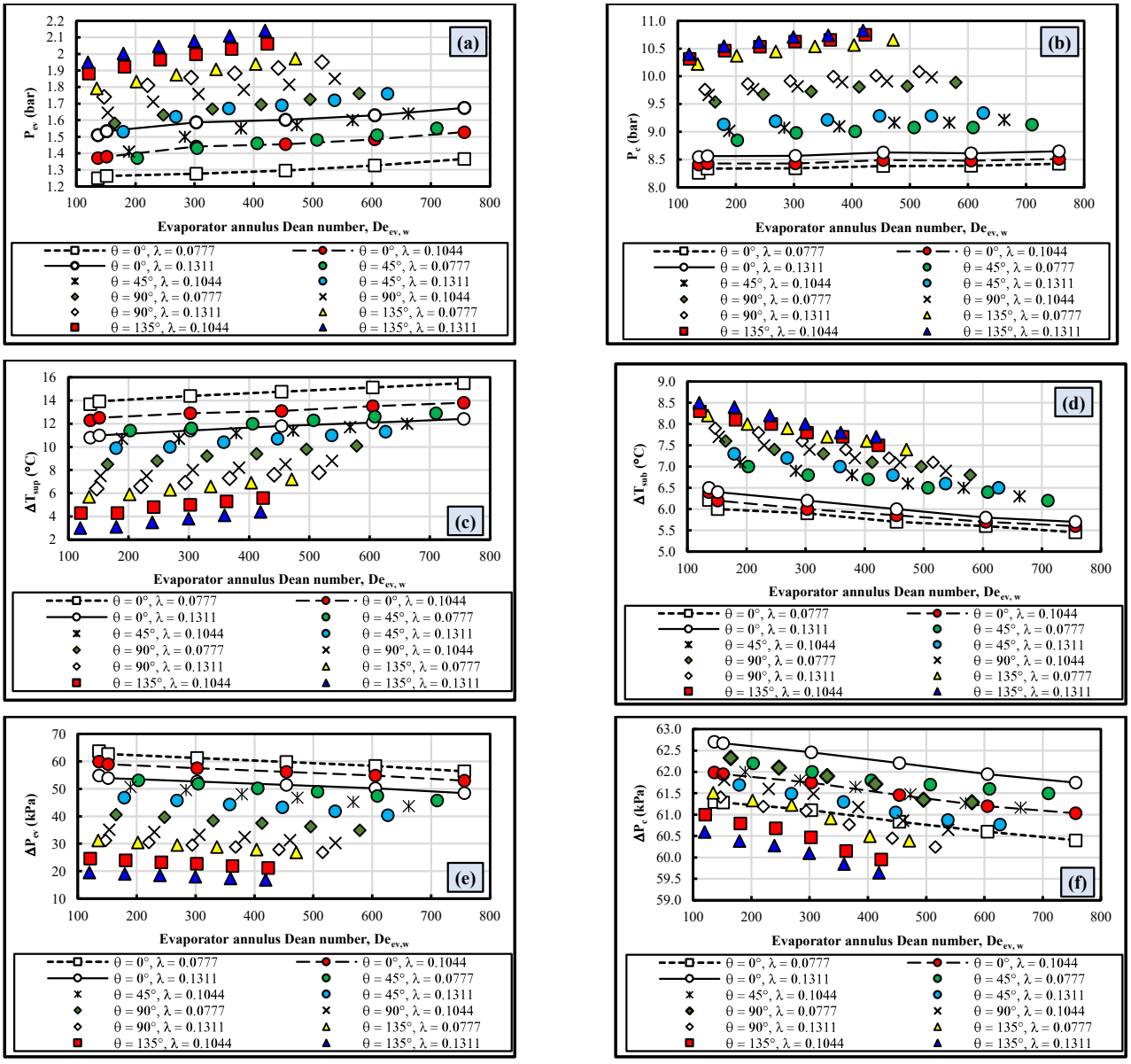

Fig. 5: Effect of CCTIT evaporator geometry on VCRS operating conditions; (a) P_{ev}, (b) P_c, (c) $\Delta T_{sup, ev}$, (d) $\Delta T_{sub, c}$, (e) ΔP_{ev}, (f) ΔP_c.

Effect of CCTIT evaporator taper angle: It is revealed from Fig. 5 that increasing the taper angle of the CCTIT evaporator leads to a significant increase in the average pressure of both the evaporator and the condenser, and in the refrigerant subcooling inside the condenser, in addition to a noticeable decrease in the superheating of the refrigerant inside the evaporator. With increasing the taper angle of the CCTIT evaporator from 0 to 135°, the evaporator and condenser average pressures increase from 1.44 bar to 1.97 bar, and from 8.47 bar to 10.55 bar, respectively. In addition, the refrigerant is superheated inside the evaporator and subcooled inside the condenser by average values of 13.1°C and 6°C, respectively, at θ_{ev} = 0° and by 5°C and 7.9°C, respectively, at θ_{ev} = 135°. Furthermore, with increasing θ_{ev} from 0 to 135°, the refrigerant average pressure loss in the evaporator decreases from 56.3 kPa to 23.4 kPa. This can be attributed to decreasing the centrifugal force in both sides of the CCTIT evaporator with increasing its taper angle (the evaporator coil mean diameter increases), which diminishes the secondary flow formation. This reduces the pressure drop in the evaporator and rises the compressor suction pressure, and consequently increases the VCRS pressures. This leads to increasing their corresponding saturation temperatures, in addition to a lower superheating temperature of the refrigerant entering the condenser with decreasing the evaporator taper angle. This slightly enhances the subcooling of the refrigerant inside the condenser, which leads also to an insignificant effect of the evaporator taper angle on the quality of the refrigerant at the evaporator inlet.

Effect of CCTIT evaporator torsion: It is observed from Fig. 5 that the effect of coil torsion is lower than that of the coil taper angle in the investigated range of these parameters. It is clear that increasing the CCTIT evaporator torsion slightly increases the average pressures of both the evaporator and condenser, in addition to the refrigerant subcooling inside the condenser, and slightly reduces the superheating of the refrigerant in the evaporator. With increasing the torsion of the CCTIT evaporator from 0.0777 to 0.1311, the evaporator and condenser average pressures increase from 1.58 bar to 1.79 bar, and from 9.4 bar to 9.6 bar, respectively. In addition, the refrigerant is superheated inside the evaporator and subcooled inside the condenser by average values of 10.6°C and 6.9°C, respectively, at λ_{ev} = 0.0777 and by 8.2°C and 7.2°C, respectively, at λ_{ev} = 0.1311. Furthermore, with increasing λ_{ev} from 0.0777 to 0.1311, the refrigerant average pressure loss in the evaporator slightly decreases from 44.2 kPa to 35.7 kPa, respectively. This can be returned to increasing the rotational force as a result of increasing the coil torsion, which diminishes the secondary flow that established by the centrifugal effect.

Effect of heating water Dean Number: It is indicated from Fig. 5 that the heating water Dean Number slightly affects the VCRS operating conditions. It is clear that with increasing $De_{ev,\,w}$, the average pressures of both the evaporator and condenser, in addition to the refrigerant superheating inside the evaporator slightly increase, while the refrigerant subcooling in the condenser slightly decreases. With increasing $De_{ev,\,w}$ from 119.8 to 756.4, the evaporator and condenser average pressures increase from 1.59 bar to 1.77 bar, and from 9.34 bar to 9.62 bar, respectively. In addition, the refrigerant is superheated inside the evaporator and subcooled inside the condenser by average values of 8.7°C and 7.4°C, respectively, at $De_{ev,\,w}$ = 119.8 and by 10.1°C and 6.6°C, respectively, $De_{ev,\,w}$ = 756.4. Furthermore, with increasing $De_{ev,\,w}$ from 119.8 to 756.4, the refrigerant average pressure loss in the evaporator slightly decreases from 42.6 kPa to 37 kPa, respectively. This can be returned to increasing the corresponding evaporator saturation temperature and pressure as a result of increasing the heating water flow rate in addition to increasing the annulus side centrifugal force.

5.2 VCRS Specifications

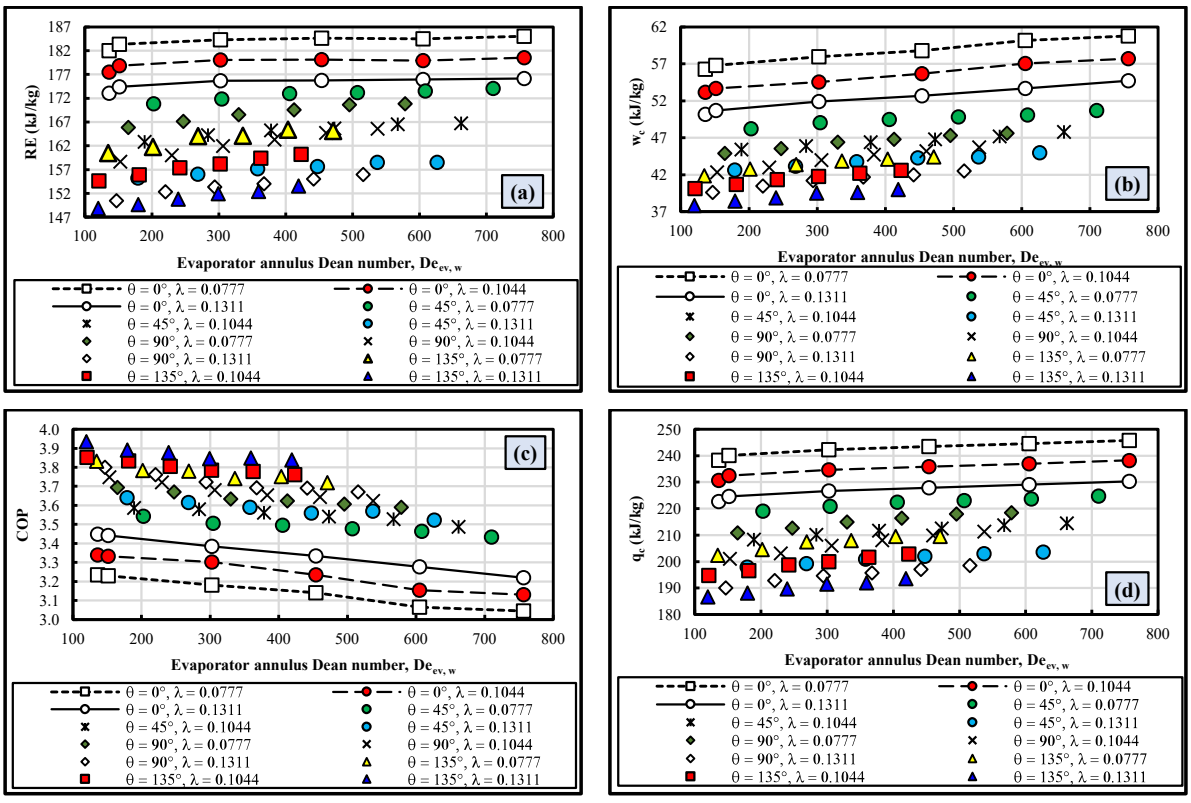

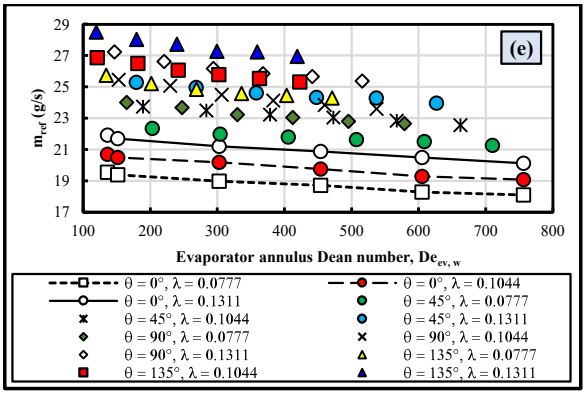

Fig. 6: Effect of CCTIT evaporator geometry on VCRS specifications; (a) RE, (b) w_c, (c) COP, (d) q_c, (e) m_{ref}.

Effect of CCTIT evaporator taper *angle:* It is evident that the CCTIT evaporator taper angle significantly affects the VCRS performance parameters as illustrated in Fig. 6. Increasing the evaporator taper angle from 0 to 135° reduces both the refrigerant RE and the compressor specific work by an average percentage decrease of 12.3% and 25.4%, respectively. This augments the COP of the VCRS by an average percentage increase of 17.4%.The decrease in the RE is due to decreasing the centrifugal force in both sides of the CCTIT evaporator with increasing the coil taper angle (the coil mean diameter increases), which diminishes the secondary flow. Therefore, the refrigerant superheating inside the evaporator decreases, which reduces the evaporator refrigeration effect. Simultaneously, the specific volume of the refrigerant at the compressor inlet decreases with decreasing the refrigerant temperature at the compressor inlet, and consequently the specific work required to compress the refrigerant molecules decreases. This is also the reason for increasing the refrigerant mass flow rate as a result of increasing the taper angle of the CCTIT evaporator. Additionally, increasing the evaporator taper angle decreases the temperature of the refrigerant at the condenser inlet, which leads to decrease the condenser load.

Effect of CCTIT evaporator torsion: It is demonstrated from Fig. 6 that the effect of coil torsion is lower than that of the coil taper angle in the investigated range of these parameters. It is clear that increasing the CCTIT evaporator torsion from 0.0777 to 0.1311 reduces both the RE and the compressor specific work by an average percentage decrease of 7.5% and 10.8%, respectively. This slightly enhances the COP of the VCRS by an average percentage of 3.5%. As mentioned before, increasing the evaporator torsion slightly reduces the refrigerant superheating inside the evaporator, which slightly minimizes the evaporator refrigeration effect. While simultaneously, the specific volume of the refrigerant at the compressor inlet decreases, and consequently the specific work required to compress the refrigerant molecules decreases. This is also the reason for the slight increase in the refrigerant mass flow rate with increasing the torsion of the CCTIT evaporator. Additionally, increasing the evaporator torsion reduces the temperature of the refrigerant at the condenser inlet, which leads to minimize the condenser load.

Effect of heating water Dean Number: It is indicated from Fig. 6that the heating water Dean Number slightly affects the VCRS specifications. It is clear that with increasing the heating water Dean Number from 119.8 to 756.4, both the RE and the compressor specific work slightly increase by an average percentage of 2.7% and 6.8%, respectively. This slightly reduces the COP of the VCRS by an average percentage of 3.7%. The slight increase in the RE is due to increasing the superheating of the refrigerant inside the evaporator with increasing the hearting water Dean Number in the CCTIT evaporator annulus, which induces more effective secondary flow. Therefore, the refrigerant superheating inside the evaporator increases, which augments the evaporator refrigeration effect. Additionally, the specific volume of the refrigerant at the compressor inlet increases with increasing hearting water Dean Number, which rises the refrigerant temperature at the compressor inlet, and consequently the specific work required to compress the refrigerant molecules increases. This is also the reason for decreasing the refrigerant mass flow rate as a result of increasing the hearting water Dean Number.

6Experimental Correlations

Using the present experimental data, an empirical correlation is developed to predict the COP of the VCRS as follows;

$$COP = 5.71\left(\frac{1+\theta_{ev}}{180}\right)^{0.029}\lambda_{ev}^{0.061}De_{ev,w}^{-0.034} \quad (17)$$

Eqs. (17) is applicable for a VCRS based on a single stage compression unit, uses R134a as the refrigerant, with CCTIT evaporator and condenser of $0° \le \theta_{ev} \le 135°$, $0.0777 \le \lambda_{ev} \le 0.1311$, $119.8 \le De_{ev,w} \le 756.4$, $1.25\ bar \le P_{ev} \le 2.14\ bar$, $8.26\ bar \le P_c \le 10.83\ bar$, and $5.06 \le (P_c/P_{ev}) \le 6.71$. A comparisons of the COP of the VCRS with those calculated by the proposed correlation is shown in Fig. 7.

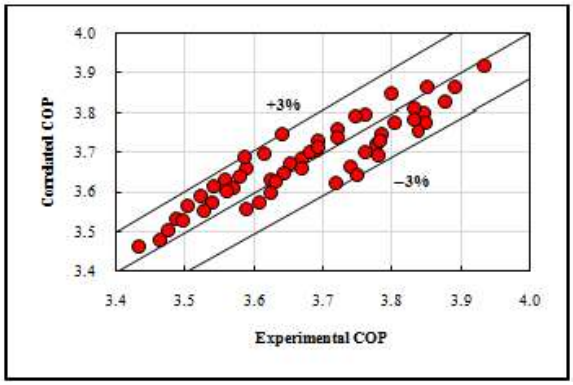

Fig. 7: Comparison of the present experimental values with that correlated by Eqs. (17).

From this figure, it is evident that the proposed correlation is in good agreement with the present experimental data. It is clearly seen that the data falls of the proposed equation within maximum deviation of $\pm 3\%$for the COP of the VCRS.

7Conclusions

The present study experimentally investigates the effect of the geometrical parameters of a CCTIT evaporator and its operating conditions on the COP of a VCRS. The CCTIT evaporator is in vertical position, through which R134a flows in its internal tube as a refrigerant, while a pure water flows in its annulus as heating mediums, in a counter-flow configuration. The investigated operating parameters $0° \le \theta_{ev} \le 135°$, $0.0777 \le \lambda_{ev} \le 0.1311$, $119.8 \le De_{ev,w} \le 756.4$, $1.25\ bar \le P_{ev} \le 2.14\ bar$, $8.26\ bar \le P_c \le 10.83\ bar$, and $5.06 \le (P_c/P_{ev}) \le 6.7$.According to the obtained results, the following conclusions can be expressed:

- Increasing the CCTIT evaporator taper angle augments the COP of the VCRS.

➢ Increasing the evaporator taper angle from 0 to 135° augments the COP of the VCRS by an average percentage increase of 17.4%.

- Increasing the CCTIT evaporator torsion augments the COP of the VCRS.

➢ Increasing the CCTIT evaporator torsion from 0.0777 to 0.1311 enhances the COP of the VCRS by an average percentage of 3.5%.

- Decreasing the CCTIT evaporator heating water Dean Number augments the COP of the VCRS.

➢ Increasing the heating water Dean Number from 119.8 to 756.4 reduces the COP of the VCRS by an average percentage of 3.7%.

- An experimental correlation is developed to predict the COP of the VCRS.

- **References**

[1] N.Q. Minh, N.J. Hewitt, and P.C. Eames, "Improved Vapour Compression Refrigeration Cycles: Literature Review and their Application to Heat Pumps", International Refrigeration and Air Conditioning Conference at Purdue, July 17–20, 2006.

[2] Z. Zhao, X. Wang, D. Che and Z. Cao, "Numerical Studies on Flow and Heat Transfer in Membrane Helical-Coil Heat Exchanger and Membrane Serpentine-Tube Heat Exchanger", International Communications in Heat and Mass Transfer, vol. 38(9), pp. 1189–1194, 2011.

[3] T.A. Pimenta and J.B.L.M. Campos, "Friction Losses of Newtonian and Non-Newtonian Fluids Flowing in Laminar Regime in a Helical Coil", Experimental Thermal and Fluid Science, vol. 36, pp. 194–204, 2012.

[4] R. Gupta, R.K. Wanchoo and T.R.M.J. Ali, "Laminar Flow in Helical Coils: A Parametric Study", Industrial & Engineering Chemistry Research, vol. 50(2), pp. 1150–1157, 2011.

[5] M.R. Salem, R.K. Ali, R.Y. Sakr, and K.M. Elshazly, "Experimental Study on Convective Heat Transfer and Pressure Drop of Water-Based Nanofluid inside Shell and Coil Heat Exchanger", PhD dissertation, Faculty of Engineering at Shoubra, Benha University, 2014. DOI: 10.13140/RG.2.2.31958.75846.

[6] S.A. Klein, D.T. Reindl and K. Brownell, "Refrigeration System Performance Using Liquid-Suction Heat Exchangers", International Journal of Refrigeration, vol. 23(8), pp. 588–596, December 2000.

[7] J. Navarro-Esbrí, R. Cabello and E. Torrella, "Experimental Evaluation of the Internal Heat Exchanger Influence on a Vapour Compression Plant Energy Efficiency Working with R22, R134a and R407C", Energy, vol. 30(5), pp. 621–636, April 2005.

[8] S.J. Inamdar and H.S. Farkade, "Performance Enhancement of Refrigeration Cycle by Employing a Heat Exchanger", International Journal of Engineering Research and Advanced Technology (IJERAT), vol. 2 (11), November 2016.

[9] R. Rakesh, H.N. Manjunath, Madhusudan, "Study of Vapour Compression Refrigeration System Using Double Pipe Heat Exchanger", International Journal of Advance Research in Science and Engineering, vol. 5(6), pp. 138–144, July 2016.

[10] Prayudi and R. Nurhasanah, "Analysis of Effect of Sub Cooling Performance of Vapour Compression Refrigeration System with Cooling Load Variation", ARPN Journal of Engineering and Applied Sciences, vol. 11(2), pp. 906–911, January 2016.

[11] B.K. Jha, K. Hire, A.O. Kori and D. Bhole, "Performance Enhancement of VCRS Using LSHX", International Journal of Modern Trends in Engineering and Research, vol. 4(1), pp. 205–209, January 2017.

[12] A.O. Elsayed, "Experimental Study on the Performance of Twisted Capillary Tube", International Refrigeration and Air Conditioning Conference at Purdue, July 17–20, 2006.

[13] M.A. Akintunde, "Effect of Coiled Capillary Tube Pitch on Vapour Compression Refrigeration System Performance", Assumption University Journal of Technology, vol. 11(1), pp. 14–22, July 2007.

[14] M.K. Khan, R. Kumar and P.K. Sahoo, "An Experimental Study of the Flow of R-134a inside an Adiabatic Spirally Coiled Capillary Tube", International Journal of Refrigeration, vol. 31, pp. 970–978, 2008.

[15] A. Poolkrajang and N. Preamjai, "Optimization of Capillary Tube in Air Conditioning System", Asian Journal on Energy & Environment, vol. 10(3), pp. 165–175, 2009.

[16] M.K. Mittal, R. Kumar and A. Gupta, "An Experimental Study of the Flow of R-407C in an Adiabatic Spiral Capillary Tube", Journal of Thermal Science and Engineering Applications, vol. 1, 041003–1, December 2009.

[17] M.K. Mittal, R. Kumar and A. Gupta, "An Experimental Study of the Flow of R- 407C in an Adiabatic Helical Capillary Tube", Department of Mechanical and Industrial Engineering, Indian Institute of Technology, Roorkee 247667, India, international journal of refrigeration, vol. 33, pp. 840–847, 2010.

[18] J.K. Dabas, A.K. Dodeja, S. Kumar, and K.S. Kasana, "Performance Characteristics of "Vapour Compression Refrigeration System" Under Real Transient Conditions", International Journal of Advancements in Technology, vol. 2(4), pp. 584–593, October 2011.

[19] A.H. Dhumal and H.M. Dange, "Investigation of Influence of the Various Expansion Devices on the Performance of a Refrigerator Using R407c Refrigerant", Int. J. Adv. Engg. Tech, vol. V(II), pp. 96–99, April-June 2014.

[20] N.N. Raja and A.D. Khanderao, "Experimental Investigation on the Effect of Capillary Tube Geometry on the Performance of Vapor Compression Refrigeration System", Asian Journal of Engineering and Applied Technology, vol. 5(2), pp. 29–35, 2016.

[21] S.V. Rao, H. Sharma, P.K. Gound, T. Walgude and S. Gavas, "Experimental Verification of Performance of Capillary Tube Using Vapour Compression Refrigeration System", International Journal of Research in Science & Engineering, vol. 3(2), March-April 2017.

[22] S. Bi, K. Guo, Z. Liu, J. Wu, "Performance of a Domestic Refrigerator Using TiO2-R600a Nano-Refrigerant as Working Fluid", Energy Conversion and Management, vol. 52, pp. 733–737, 2011.

[23] N. Subramani and M.J. Prakash, "Experimental Studies on a Vapor Compression System Using Nano Refrigerants", International Journal of Engineering, Science and Technology, vol. 3(9), pp. 95–102, 2011.

[24] D.S. Kumar and R. Elansezhian, "Experimental Study on Al2O3-R134a Nano Refrigerant in Refrigeration System", International Journal of Modern Engineering Research (IJMER), vol. 2(5), pp. 3927–3929, Sep. –Oct. 2012.

[25] R. Reji Kumar, K. Sridhar and M. Narasimha, "Heat Transfer Enhancement in Domestic Refrigerator Using R600a/Mineral Oil/Nano-Al2O3 as Working Fluid", International Journal of Computational Engineering Research, vol. 3(4), pp. 42–50, April 2013.

[26] R. Reji Kumar, M. Narasimha and K. Sridhar, "Heat Transfer Enhancement in Air Conditioning System Using Nanofluids", International Journal of Research in Computer Application & Management, vol. 3(5), pp. 120–126, May 2013.

[27] I.M. Mahbubul, R. Saidur and M.A. Amalinaa, "Heat Transfer and Pressure Drop Characteristics of Al2O3-R141b Nanorefrigerant in Horizontal Smooth Circular Tube", Procedia Engineering, vol. 56, pp. 323–329, 2013.

[28] K. Singh and K. Lal, "An Investigation into the Performance of a Nanorefrigerant (R134a+Al2O3) Based Refrigeration System", International Journal of Research in Mechanical Engineering & Technology, vol. 4(2), pp. 158–162, 2014.

[29] T. Coumaressin and K. Palaniradja, "Performance Analysis of a Refrigeration System Using Nano Fluid", International Journal of Advanced Mechanical Engineering, vol. 4(5), pp. 521–532, 2014.

[30] A. Senthilkumara and R. Praveenb, "Performance Analysis of a Domestic Refrigerator Using Cuo–R600a Nano–Refrigerant as Working Fluid", Journal of Chemical and Pharmaceutical Sciences, JCHPS Special Issue 9, pp. 30–33, April 2015.

[31] V.K. Dongare, J. Kadam, A. Samel, R. Pawar and S. Sarvankar, "Enhancement of Vapour Compression Refrigeration System using Nanofluids", International Research Journal of Engineering and Technology (IRJET), vol. 4(4), pp. 2218–2225, 2017.

[32] R.S. Mishra, "Vapour Compression Refrigeration Systems Using Nano Materials Mixed with R718 in Secondary Circuit of Evaporator for Enhancing Thermodynamic Performances", International Journal of Research in Engineering and Innovation, vol. 1(3), pp. 37–48, 2017.

[33] V.P. Mohod and N.W. Kale, "Experimental Analysis of Vapour Compression Refrigeration System Using Nanorefrigerant", Proceedings of 68th IRF International Conference, 29th January 2017, Pune, India.

[34] T. Kanthimathi, A. Teja and D.P. Saradhi, "Enhancement of Heat Transfer Using Nano-Refrigerant", International Journal of Pure and Applied Mathematics, vol. 115(7), pp. 349–354, 2017.

[35] M.K. Krishna Prasonna and P.S. Kishore, "Enhancement of COP in a Vapour Compression Refrigeration System", International Journal of Engineering Research & Technology, vol. 3(11), pp. 1535–1539, November 2014.

[36] J. Chandramouli, C. Sreedhar and E.V. Subbareddy, "Design, Fabrication and Experimental Analysis of Vapour Compression Refrigeration System with Ellipse Shaped Evaporator coil", International Journal of Innovative Research in Science, Engineering and Technology, vol. 4(8), pp. 7775–7782, August 2015.

[37] B.S. Kumar, A.R. Reddy, C. Ramanjaneylulu and N.J. Krishna, "Experimental Investigation on a Vapour Compression Refrigeration System with a Spiral Shaped Condenser", International Journal of Research in Mechanical Engineering, vol. 2(2), pp. 11–14, 2015.

[38] R.H. Vali, P. Yagnasri and S.N.K. Reddy, "Performance Analysis of VCR System with Varying the Diameters of Helical Condenser Coil by Using R-134a Refrigerant", International Journal of Engineering Sciences & Research Technology, vol. 5, pp. 872–883, February 2016.

[39] S. Patil, S. Patil, Y. Patil, N. Pawar and V. Ugare, "Performance Analysis of Vapour Compression Refrigeration System with Spiral Micro-tube Condenser", International Journal of Scientific & Engineering Research, vol. 8(4), pp. 136–140, April 2017.

Nomenclatures

Cp	Specific heat at constant pressure, J/kg.℃
d	Diameter, m
h	Specific enthalpy, kJ/kg
I	Electrical current, A
L	Length, m
ṁ	Mass flow rate, kg/s
p	Pitch, m
P	Pressure, Pa
q	Specific heat, kJ/kg
Q	Heat transfer rate, W
T	Temperature, ℃ or K
V	Voltage drop, V
w	Specific work, kJ/kg
W	Power, W

Dimensionless Groups

De	Dean Number
Re	Reynolds number

Greek Letters

Δ	Differential
δ	Coil curvature ratio
∅	Power factor
λ	Coil torsion (pitch ratio)
π	Pi ≡ A mathematical constant ≅ 3.1416

Superscripts and Subscripts

ave	Average
c	Condenser/compressor
ev	Evaporator
i	Inner or inlet or internal
o	Out or outer
ref	Refrigerant
s	Surface
sub	Subcooled/subcooling
sup	Superheated/superheating
t	Tube
w	Water

Acronyms and Abbreviations

AC	Alternate Current
CCTIT	Conically Coiled Tube-In-Tube
COP	Coefficient Of Performance
HCT	Helically Coiled Tube
HCTIT	Helically Coiled Tube-In-Tube
PVC	Polyvinyl Chloride
RE	Refrigeration Effect
VCRS	Vapour Compression Refrigeration System